Green Chemistry

Accepted Manuscript

ROYAL SOCIETY OF CHEMISTRY

www.rsc.org/greenchem

Graphical Abstract

Structured nanoporous-gold/Al-fiber: Galvanic deposition preparation and reactivity for oxidative coupling of methanol to methyl formate

Qiaofei Zhang, Yakun Li, Li Zhang, Li Chen, Ye Liu and Yong Lu*

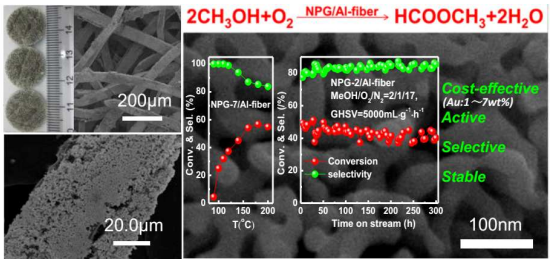

Microfibrous-structured nanoporous gold (NPG) on Al-fiber catalysts are developed with the aid of galvanic deposition method using a 3D network of 50μm-Al-fiber as substrate, which are cost-effective, highly active/selective and stable for oxidative coupling of methanol to methyl formate.

Cite this: DOI: 10.1039/c0xx00000x

www.rsc.org/xxxxxx

ARTICLE TYPE

Structured nanoporous-gold/Al-fiber: Galvanic deposition preparation and reactivity for oxidative coupling of methanol to methyl formate

Qiaofei Zhang, Yakun Li, Li Zhang, Li Chen, Ye Liu and Yong Lu*

Received (in XXX, XXX) Xth XXXXXXXXX 20XX, Accepted Xth XXXXXXXXX 20XX

DOI: 10.1039/b000000x

Microfibrous-structured nanoporous gold (NPG) on Al-fiber catalysts, obtained by galvanic deposition onto a 3D network using 50µm-Al-fiber, are cost-effective (low Au-loading, *e.g.*, 1 wt%), highly active/selective (>90% selectivity at >50% conversion) and stable (at least 300 h without NPG sintering) for oxidative coupling of methanol to methyl formate.

Methyl formate is an important commodity chemical, using as solvent, environmentally friendly blowing agent, and precursor for formic acid, formamide, and dimethyl formamide.[1] The current industrial process for methyl formate production is based on the homogeneous carbonylation of methanol in the presence of sodium methoxide (a caustic liquid base) catalyst, using ultra-highly purified CO as feedgas (H_2O- and CO_2-free).[2] This method generally links to higher risk of environmental issues and faces serious problems in product separation, obviously conflicting the concept of green chemistry.[3] There is thus an urgent need to develop greener method, aimed at using solid catalysts under heterogeneous conditions.

In this context, the oxidative coupling of methanol (OCM) to methyl formate (MF) is attractive as a simple and environmentally benign process. In addition, the flourishing of methanol economy generates a further impetus to explore the OCM process, which is superior to other routes for methanol conversion and utilization regarding the extension of methanol industrial chain. Several catalysts, including non-noble metal oxides (such as SnO_2-Mo_2O_3, V_2O_5-TiO_2 and Fe_2O_3/SiO_2),[4] heteropoly acids (HPAs)[5] and noble metal systems,[6] have been extensively investigated in OCM reaction. However, their practical applications are particularly challenging. Besides concerns on the catalytic performance, thermal conductivity of the catalysts is also an important consideration because of the strong exothermicity of the OCM process. The metal oxide catalysts as well as HPAs are not active and/or selective enough from the industrial standpoint and their poor thermal conductivity will cause heat transfer limitation. Graphene-supported Ag-Pd nanocatalysts, with good heat conductivity, is reported to show excellent low-temperature activity and selectivity,[6] delivering 90% conversion and 100% selectivity at 70 °C.

Recently, nanoporous gold (NPG) has attracted increasing attention because of its wide range of applications including catalysis,[7] cell imaging,[8] energy storage/transformation,[9] and development of chemical sensors.[10] Fabricated by selectively leaching silver from Ag-Au alloys, NPG possesses high

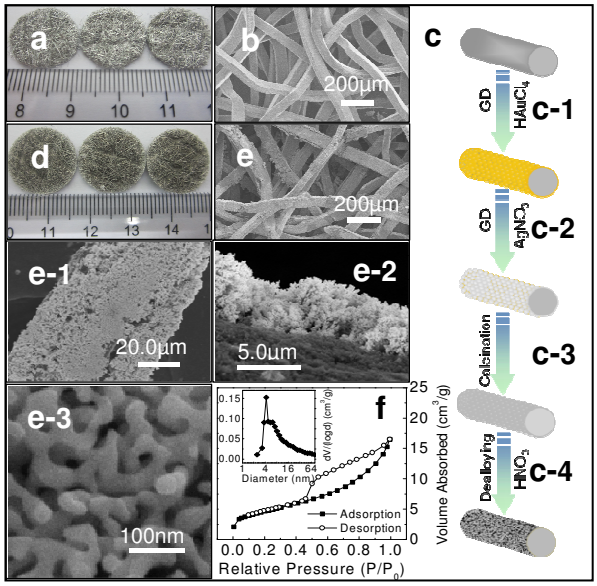

Fig. 1 Galvanic deposition (GD) preparation and structural features from micro- to macro-scale. Photograph (a) and SEM image (b) of Al-fiber substrate. (c) Preparation schematic illustration (stepwise galvanic deposition of Au and Ag at Au/Ag weight ratio of 45/55; alloying is at 300 °C in He for 2 h; Ag leaching at room temperature for 24 h, using 65 wt% HNO_3 solution). Photograph (d), SEM (e), and N_2 adsorption-desorption isothermal and Barrett–Joyner–Halenda (BJH) mesopore size (f) for the representative NPG-7/Al-fiber catalyst.

thermal/electrical conductivity, three-dimensional nanostructure, much larger characteristic lengths both in ligament and nanopore diameters.[11] Owing to an abundance of surface defects and residual Ag, the bulk NPG exhibits excellent catalytic performance in some important reaction processes[7,12] such as the OCM to MF. Most notably, the bulk NPG provides high resistance to sintering compared to the Au-NPs catalysts, which is an important consideration for practical applications.[7] However, high cost of the bulk NPG hampers its practical application as catalyst for OCM process.

In this communication, we present a cost-effective microfibrous-structured NPG on Al-fiber catalyst system for the OCM to MF. The NPG/Al-fiber catalysts are obtained in macro-scale by galvanically depositing Au-Ag alloy onto a thin-sheet 3-dimensional (3D) network structure using 50µm-Al-fiber followed by Ag-leaching. Methanol conversion of >50% is achieved with a MF selectivity of >90% at 150 °C, using a feedgas of $MeOH/O_2/N_2$=2/1/17 (10 vol% methanol). The

Table 1. OCM to MF, catalysed by NPG/Al-fiber catalysts

Catalyst	[Au]/[Ag] [a] (wt%)	S_{BET} (m^2/g)	S_{NPG} [b] (m^2/g)	X [c] (%)	S [c] (%)	TOF (s^{-1}) [d]
NPG-7/Al-fiber	7.1/0.6(5.6/6.8)	16	14	50	94[e]	0.4
NPG-4/Al-fiber	3.9/0.3(2.8/4.5)	9	7	32	95[e]	0.9
NPG-2/Al-fiber	1.9/0.2(1.2/2.7)	9	7	15	100	0.9
NPG-1/Al-fiber	1.0/0.1(0.9/1.7)	8	6	8	100	1.1
Bulk NPG[f]	99/1(30/70)	7	7	50[g]	91[e,g]	0.2

[a] Data in and out the parenthesis are the Au-/Ag-loading in NPG/Al-fiber samples before and after Ag leaching for 24 h, determined by inductively coupled plasma-atomic emission spectrometry (ICP-AES). [b] S_{NPG}: surface area of NPG, assuming to be the mesopore surface area. [c] Methanol conversion (X) and MF selectivity (S) at 140 °C (0.2 g Cat., $MeOH/O_2/N_2$ =2/1/17 (10 vol% methanol), GHSV = 5000 mL $g_{cat.}^{-1}$ h^{-1},). [d] Turnover Frequency (TOF, mol_{MF} $mol_{surf.-Au}^{-1}$ h^{-1}) based on MF yield and surface Au (ESI† for detail). [e] CO_2 is dominant byproduct and CH_2O is trace. [f] Bulk NPG is prepared by etching of Ag-Au alloys in conc. nitric acid (HNO_3, 65 wt%) by free corrosion. [g] Using 0.05 g bulk NPG diluted with 25–50 mesh quartz sand (0.15 g).

catalyst is stable for at least 300 h without NPG sintering. Gold loading can be reduced down to 1 wt% without unacceptable reactivity decline. Leaching of Ag is essential for the OCM selectivity of the NPG/Al-fiber catalysts, by nature, playing a key role in constructing the 3D nanopore structure and tuning the surface O species.

Fig. 1 shows the preparation strategy and the structural features from micro- to macro-scale of the representative NPG/Al-fiber catalysts. The specific surface area, Au loading, and Au dispersion of the NPG/Al-fiber samples are collected in Table 1. A microfibrous structure consisting of 10 vol% 50μm-aluminium-fiber and 90 vol% void volume, with thin-sheet form and characteristic irregular 3D networks (Fig. 1a and 1b), is employed as substrate. Stepwise deposition of Au and Ag onto the Al-fiber is realized with the aid of galvanic exchange reaction (denoted as galvanic deposition [GD]; Fig. 1c-1 and 1c-2). Note that the GD processes can automatically proceed as soon as Al-fibers is wetted by $HAuCl_4$ or $AgNO_3$ aqueous solution at room temperature, due to the large electrode potential difference between the Al^{3+}/Al^0 (-1.6 V) and $[AuCl_4]^-/Au^0$ (1.0 V) or Ag^+/Ag^0 (0.8 V) pairs. Alloying of Au-Ag is facile,[13] which can proceed by calcining the samples at 300 °C (Fig. 1c-3). After that, gold contents in the Au-Ag alloys are measured by ICP-AES, for all the resulting Au-Ag/Al-fiber samples, to be ~45 wt%. This meets the criteria on Au content in Au-Ag alloy for getting nanopore structure by Ag-leaching, since no porosity evolution can be observed as Au content is higher than 50 wt% for the Au-Ag alloy system according to Bischoff *et al.*[14,15]

Subsequently, the Au-Ag/Al-fiber sample is immersed into a 65% HNO_3 aqueous solution to selectively leach Ag from Au-Ag alloy for desired time length (*e.g.*, 24 h) at room temperature (Fig. 1c-4) while the passivation of Al-fiber surface automatically proceeds thereby avoiding the dissolving of Al-fiber. As a result, NPG/Al-fiber catalysts are obtained with a well-preserved thin-sheet structure (Fig. 1d). Clearly, for the representative NPG-7/Al-fiber catalyst (Au: 7.1 wt%, Table 1), a very uniform NPG shell (~5 μm thick) is formed along with the Al-fiber (Fig. 1e). High magnitude SEM image shows that the supported NPG exhibits 3D nanopore structure almost same as the reported bulk NPG[11,16] (Fig. 1e-3). Notably, when reducing Au loading to or lower than 3 wt%, NPG islands are formed instead of the uniform shell (Fig. S1, ESI†). The NPG-7/Al-fiber presents a N_2-BET specific surface area of 16 m^2/g and shows mesopore feature evidenced by the step at P/P_0 of 0.4~0.6 on the N_2 adsorption-desorption isothermal with a Barrett–Joyner–Halenda (BJH) mesopore size of 4~8 nm (Fig. 1f).

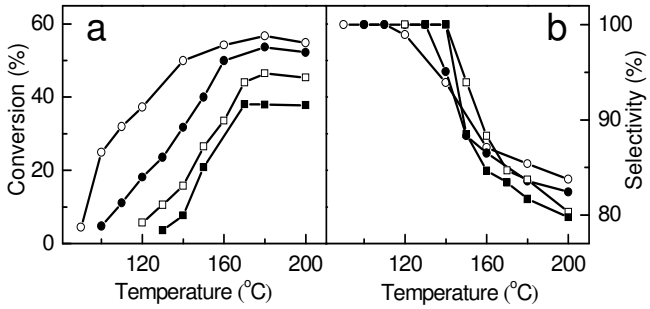

Fig. 2 Methanol conversion (a) and methyl formate selectivity (b) for temperature-dependent OCM over NPG/Al-fiber catalyst with varied Au loadings of 1 wt% (■), 2 wt% (□) and 4 wt% (●)7 wt% (○). Reaction conditions: 0.2 g Cat., $MeOH/O_2/N_2$=2/1/17, GHSV=5000 mL $g_{cat.}^{-1}$ h^{-1}.

We initially investigated the effect of Au loading on the catalytic performance of NPG/Al-fiber in OCM to MF (Table 1). At 140 °C, the MF selectivity (>90%) is almost independent on the Au loading but not the methanol conversion. The NPG-7/Al-fiber catalyst delivers the highest methanol conversion of 50%, outperforming the NPG-1/Al-fiber by at least 5-fold. Note that the catalysts all provide a TOF of 0.4~1.1 s^{-1}, indicating almost equivalent intrinsic activity. This observation is not surprising because of the similarity in nanostructure and composition of NPG in all the cases (Table 1, Fig. 1 and Fig. S1). Yet, TOF for the bulk NPG is obtained to be 0.2 s^{-1} under identical reaction conditions.

Fig. 2 shows the temperature dependence of OCM conversion and selectivity for the representative NPG/Al-fiber catalysts. Similar conversion and selectivity evolution behaviours are observed with the temperature in all cases. The NPG-7/Al-fiber offers higher conversion than other ones in the whole temperature range tested. The methanol conversion shows a dramatic increase indicative with increasing temperature to 160 °C, and then almost remains constant with further increasing temperature to 200 °C. The MF selectivity shows reverse evolution behaviour along with the increase of temperature. Notably, for OCM using NPG/Al-fiber, high Au loading is required for achieving low-temperature activity while elevated reaction temperature is needed for low-Au-loading catalysts to delivery good reactivity. At 100 °C, the NPG-7/Al-fiber is capable of achieving ~100% MF selectivity with ~25% methanol conversion of a feed of 10% methanol at a GHSV of 5000 mL $g_{cat.}^{-1}$ h^{-1}. With increasing temperature to 180 °C, high methanol conversion of 57% is obtainable over this catalyst but MF selectivity declines to 85% (intermediate CH_2O accounts for 10% and undesired combustion to CO_2 for the remaining 5%). Over the NPG-1/Al-fiber (Au: only 1 wt%), a conversion of 35% still can be obtained with an MF selectivity of 85% at 160 °C. In addition, two Ag-7/Al-fiber and Au-7/Al-fiber catalysts are also prepared by GD method and are tested in OCM reaction process. Both of them, with the bulk-like Ag and Au on the Al-fibers, are inactive for the OCM to MF, strongly confirming that the nanoporous structure is essential to the OCM reaction process.[16]

As previously noted, the bulk NPG is active (10% conversion)

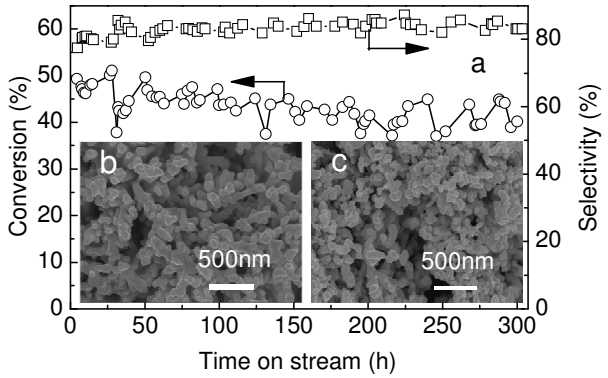

Fig. 3 (a) Methanol conversion and MF selectivity for the OCM to MF vs time on stream using NPG-2/Al-fiber catalysts (0.2 g Cat., $MeOH/O_2/N_2$ =2/1/17 (10 vol% methanol), 170 °C, GHSV=5000 mL $g_{cat.}^{-1}$ h^{-1}). SEM images of NPG-2/Al-fiber: (b) after 300 h on stream and (c) fresh.

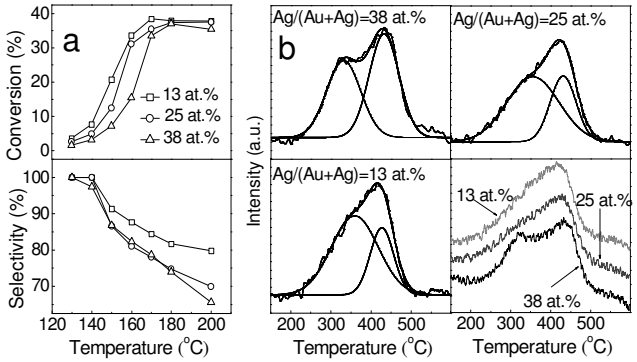

Fig. 4 (a) Methanol conversion and MF selectivity for OCM to MF vs Ag residual contents for NPG-1/Al-fiber catalysts (0.2 g Cat., $MeOH/O_2/N_2$=2/1/17 (10 vol% methanol, GHSV=5000 mL $g_{cat.}^{-1}$ h^{-1}). (b) O_2-TPD profiles of the catalyst samples after reaction.

and selective (100% MF selectivity) even at room temperature while a high conversion of 60% is obtainable with 97% MF selectivity only at elevated temperature of 80 °C.[16] In addition, during a 17-day testing at 60 °C, the bulk NPG catalyst shows a continuous decline in conversion with a rate of ~6% per 24 h.[16] More recently, $Au_{2.0}$-$Pd_{1.0}$/graphene catalyst is reported to be active and stable for methanol conversion (85~90%) with 100% selectivity at 70 °C for 48 h running.[6] However, these catalysts are far away from the practical applications, because of the high cost, the low methanol concentration (1.0~6.4 vol%) and/or the challenge of regeneration.

Besides the significant reduction of gold loading, our NPG/Al-fiber catalysts demonstrate superior stability over the above mentioned catalyst system. A long-term test on the NPG-2/Al-fiber catalyst for the OCM to MF is carried out at 170 °C using GHSV of 5000 mL $g_{cat.}^{-1}$ h^{-1}. The catalyst is stable for at least 300 h, showing excellent conversion (~45%) and selectivity (~85%) maintenance through the entire testing (Fig. 3a). Not surprisingly, the NPG for the used catalyst still preserves its 3D nanostructure very well (Fig. 3b) with surface area of 8 m^2/g, being almost unchanged compared to the fresh catalyst (Fig. 3c). Another advantage of this catalyst is that its excellent heat conductivity can rapidly dissipate a large quantity of reaction heat from such strongly exothermic oxidation reaction. A very low ΔT (between the bed and reactor external wall) of ~15 °C was observed through the entire 300 h test. Isothermal operation is not only a safety consideration but a very important feature that benefits activity and selectivity maintenance.[17]

As previously noted, the activity and selectivity for bulk NPG are very sensitive to the Ag residual content.[16,18] Whether the chemical feature exhibits the tuning ability for the reactivity of the NPG/Al-fiber catalysts and to what extent, however, is not clear. To gain insight on it, we investigate the OCM on the samples exhibiting the same morphology but varied Ag residual contents tuned from 13 at.% (almost cannot be reduced further by prolonging the leaching time in present work) to 38 at.% (by ICP-AES) for NPG-1/Al-fiber by controlling the extent of Ag leaching. As shown in Fig. 4a, both selectivity and activity (especially at middle range temperatures) is dependent on the Ag residual content. In temperature ranged from 140 to 180 °C, the selectivity to MF declines visibly along with increasing the Ag residual content from 13 at.% to 25 at.% and then remains almost unchanged from 25 at. % to 38 at.% while the methanol conversion decreases continuously. The higher Ag residual content causes a loss of selectivity bigger than the lower Ag content as the reaction temperature increases: [97% (140 °C)→66% (200 °C)] for 38 at.% Ag *vs* [100% (140 °C)→80% (200 °C)] for 13 at.% Ag.

Temperature-programmed desorption (TPD) experiments are performed and dual-peak profiles are obtained on all the samples with varied Ag residues with almost equivalent peak areas (i.e., equivalent amount of desorbed O_2) (Fig. 4b, Table S1). Most interestingly, as the Ag residual content decreases, the low-temperature O_2-TPD peak (centred at ~340 °C) increases slightly while the high-temperature peak (centred at 435 °C) shows a downward trend (Fig. 4b, Table S1). By correlating the findings with the above reaction results, it is rational to infer that surface O species desorbed at ~340 °C are selectively active for OCM reaction and ones desorbed at ~435 °C is inactive at low reaction temperature (*e.g.*, 140 °C) but active for deep oxidation at high reaction temperature (*e.g.*, 200 °C).

Conclusions

Cost-effective, highly active/selective and stable NPG on Al-fiber catalysts are developed for OCM to MF. The NPG/Al-fiber catalysts are obtainable by galvanically depositing Au-Ag alloy onto a 3D network structure using 50μm-Al-fiber followed by Ag-leaching. Gold loading can be reduced down to 1 wt% without unacceptable reactivity decline. The catalyst is stable for at least 300 h without association of NPG sintering. Lowering Ag residual content is essential for higher selectivity of OCM, by nature, decreasing the amount of unselective surface O species. We expect that our findings will pave the way to innovative applications of NPG in the near future.

This work is funded by the "973 program" (2011CB201403) from the MOST of China, and the NSF of China (21273075, 21076083, 20973063).

Experimental Section

Catalyst preparation

The thin-sheet 3-dimensional (3D) sinter-locked network structure using 50μm-Al-fiber is employed as support, which is

purchased from Shanghai Xincai Screen Manufacturing Co. Ltd. Prior to stepwise galvanic deposition, the microfibrous-structured 50μm-Al-fiber substrate is cleaned by immersing it in a sodium hydroxide (1 wt% NaOH) aqueous solution at room temperature for removing the Al_2O_3 film.

Gold and silver are stepwise deposited onto the Al-fiber surface of the microfibrous substrate with the aid of galvanic exchange reaction. First, gold is galvanically deposited onto the cleaned Al-fiber by impregnating it with an aqueous solution containing the specified amount of $HAuCl_4$ at room temperature. The solution gradually turns from a bright yellow color to colorless within 30 min. The resulting sample is washed with distilled water until to no chloride ion to obtain Au/Al-fiber sample. Subsequently, silver is placed onto the Au/Al-fiber sample again with the aid of galvanic exchange reaction of Ag^+ with Al, by impregnating the Au/Al-fiber with an aqueous solution containing the specified amount of $AgNO_3$ at room temperature. After that, alloying of Au and Ag deposited onto the Al-fiber is performed by calcining the samples at 300 °C under the inert helium atmosphere for 2 hours to give Au-Ag/Al-fiber. At last, the Au-Ag/Al-fiber samples are immersed into a 65% HNO_3 aqueous solution to selectively leach Ag from Au-Ag alloy for desired time length (*e.g.*, 24 h if not specified) at room temperature while the passivation of Al-fiber surface automatically proceeds thereby avoiding Al-fiber dissolving.

Characterization

The NPG/Al-fiber catalysts are characterized by a scanning electron microscope (SEM, Hitachi S-4800). Specific surface area is determined from N_2 adsorption isotherm using standard Brunauer-Emmett-Teller (BET) theory on a Quantachrome Autosorb-3B instrument. The pore size distribution and total pore volume are determined using the BJH method. Temperature programmed desorption (TPD) was performed on a Quantachrome ChemBET 3000 chemisorption apparatus with a TCD and an online Mass Spectrometer (Proline Dycor, AMETEK Process Instrument, USA). The amounts of Au and Ag for the NPG/Al-fiber catalysts are quantitatively determined by inductively coupled plasma atomic emission spectrometry (ICP-AES) on a USA Thermo IRIS Intrepid Ⅱ XSP ICP spectrometer.

Reactivity tests

The gas-phase selective oxidation of methanol on these catalysts with molecular oxygen was performed on a fixed-bed quartz tube reactor (600 mm length by 16 mm inner diameter) under atmospheric pressure. Circular chips (16.1 mm diameter) of the microfibrous-structured NPG/Al-fiber catalysts are punched down from their large sheet sample and packed layer-up-layer into the tube reactor. The catalyst used in testing experiments is 0.2 g. Notice that the 0.1 mm larger diameter than the inner diameter of the tubular reactor was deliberately retained to avoid the appearance of a gap between the reactor wall and the edges of the catalyst chips, thereby preventing gas bypass. A gaseous mixture of $MeOH/O_2/N_2$ (2/1/17; 10 vol% methanol) is employed as feedstock. Such feed is obtained by controlling oxygen (oxidant, 5 ml/min) and nitrogen (diluted gas, 85 ml/min) to pass through a methanol vapor saturator prior to feeding into the catalytic bed. Two calibrated mass flow controllers are used to control the oxygen and nitrogen gas. The methanol vapor saturator is immersed into a water bath precisely controlled at 20 °C. The product effluent as well as the methanol concentration in feed mixture is analyzed online by an HP 6850 gas chromatography chromatograph equipped with thermal conductivity detector (TCD) connected to Porapak Q and MS 5A parallel capillary column (DIKMA). The gas pipeline and sampling 6-way valve between the reactor outlet and the GC injector are heated to ensure the effluent completely evaporated.

Notes and references

Shanghai Key Laboratory of Green Chemistry and Chemical Processes, Department of Chemistry, East China Normal University, Shanghai 200062, P.R. China. Fax: +86 21 62233424; Tel: +86 21 62233424; E-mail: ylu@chem.ecnu.edu.cn

† Electronic Supplementary Information (ESI) available: Supplementary text for TOF calculation; Fig. S1, Table S1. See DOI: 10.1039/b000000x/

1 Ullmann's Encyclopedia of Industrial Chemistry (Wiley, New York, ed. 7, 2009).
2 G.A. Olah, A. Goeppert and G.K.S. Prakash, Beyond oil and gas: the methanol economy. 2nd ed. Weinheim: Wiley-VCH Verlag GmbH & Co. KGaA, 2009.
3 P.T. Anastas and J.C. Warner, Green Chemistry: Theory and Practice, 1998.
4 A. Mamoru, *J. Catal.*, 1982, **77**, 279; A.S. Elmi, E. Tronconi, C. Cristiani, J.P. Gomez, P. Forzatti and G. Busca, *Ind. Eng. Chem. Res.*, 1989, **28**, 387; C. Wang and R.J. Willey, *J. Catal.*, 2001, **202**, 211.
5 H.C. Liu and E. Iglesia, *J. Catal.*, 2004, **223**, 161.
6 R. Wang, Z. Wu, C. Chen, Z. Qin, H. Zhu,G. Wang, H. Wang, C. Wu, W. Dong, W. Fan and J. Wang, *Chem. Commun.*, 2013, **49**, 8250.
7 X. Zhang and Y. Ding, *Catal. Sci. Technol.*, 2013, **3**, 2862; Y. Ding, M.W. Chen and J. Erlebacher, *J. Am. Chem. Soc.*, 2004, **126**, 6876.
8 S. Shukla, A. Priscilla, M. Banerjee, R. Bhonde, J. Ghatak, P.V. Satyam and M. Sastry, *Chem. Mater.*, 2005, **17**, 5000; O.V. Shulga, K. Jefferson, A.R. Khan, V.T.D'Souza, J. Liu, A.V. Demchenko and K.J. Stine, *Chem. Mater.*, 2007, **19**, 3902.
9 S. Gregory, R. Torsten and R. Burkhard, *J. Electroanal. Chem.*, 2002, **526**, 125.
10 M. Hieda, R. Garcia, M. Dixon, T. Daniel, D. Allara and M. Chan, *Appl. Phys. Lett.*, 2004, **84**, 628; N.V. Lavrik, C.A. Tipple, M.J. Sepaniak and P.G. Datskos, *Biomed. Microdevices*, 2001, **3**, 35; X.Y. Wang, H. Zhong, Y. Lv and H.Y. Chen, *Chem. Lett.*, 2003, **32**, 1054.
11 E. Seker, M.L. Reed and M.R. Begley, *Materials*, 2009, **2**, 2188.
12 Z. Roswitha, L. Tang, S. Karl, S. Joshua and J. Erlebacher, *J. Catal.*, 2008, **253**, 132.
13 K. Dick, T. Dhanasekaran, Z. Zhang and D. Meisel, *J. Am. Chem. Soc.*, 2002, **124**, 2312; G.W. Nyce, J.R. Hayes, A.V. Hamza and J.H. Satcher Jr, *Chem. Mater.*, 2007, **19**, 344.
14 X. Lu, E. Bischoff, R. Spolenak and T. Balk, *Scripta Mater.*, 2007, **56**, 557.
15 C. Ji and P. Searson, *Appl. Phys. Lett.*, 2002, **81**, 4437.
16 A. Wittstock, V. Zielasek, J. Biener, C.M. Friend and M. Bäumer, *Science*, 2010, **327**, 319.
17 G.F. Zhao, H.Y. Hu, M.M. Deng and Y. Lu, *Chem. Commun.*, 2011, **47**, 9642; G.F. Zhao, M.M. Deng, Y.F. Jiang, H.Y. Hu, J. Huang and Y. Lu, *J. Catal.*, 2013, **301**, 46.
18 T. Fujita, P. Guan, K. McKenna, X. Lang, A. Hirata, L. Zhang, T. Tokunaga, S. Arai, Y. Yamamoto, N. Tanaka, Y. Ishikawa, N. Asao, Y. Yamamoto, J. Erlebacher and M. Chen, *Nature Mater.*, 2012, **11**, 775.